

Application of the ZVS-PWM Commutation Cell to a Full-Bridge DC-DC Converter

Denizar C. Martins **Ivo Barbi**
 Federal University of Santa Catarina
 Department of Electrical Engineering
 Power Electronics Institute
 P. O. Box 5119
 88040-970 Florianópolis, Santa Catarina, Brazil
 Telephone: 55-48-231-9674
 FAX: 55-48-231-9770

Fernando C. Castaldo¹
 UNIUI Regional University
 Department of Technology
 Electrical Engineering Nucleus
 Rua São Francisco 501
 98700-000 Ijuí, Rio Grande do Sul, Brazil
 Telephone: 55-55-332-6100
 FAX: 55-55-332-3717

Abstract

This paper presents the analysis and design procedures of a new DC-DC Full Bridge PWM converter, using the ZVS-PWM commutation cell to achieve soft switching. Experimental results obtained from a laboratory prototype rated 1500 W are also presented. It is demonstrated that the inclusion of the auxiliary switches do not modify the PWM switching pattern. Bench tests on the prototype confirm that the proposed circuit exhibits high efficiency and behaves as a constant voltage source over an extended power output range.

1. Introduction

In the recent past the increase of the switching frequency have been intensively used in DC-DC converters as a procedure to improve the power density of such converters. However, many intrinsic characteristics of the available semiconductor devices limits in practice the switching frequency. A number of new techniques [1] have been proposed to overcome that limitation. Among them, the use of auxiliary commutation circuits promotes soft switching with reduced stresses on the semiconductor devices, achieving higher switching frequency. Regardless that characteristics, the auxiliary commutation circuits can also be applied in PWM converters without modification on the switching pattern, since the auxiliary circuits are made active only during the switching intervals [2,3,4]. Although more devices are necessary to build a converter with soft switching, the power processed by the auxiliary switches are low in comparison with the total processed power and the EMI level is reduced [5,6], leading to a high interest in such techniques.

The ZVS-PWM commutation cell [7,8] was used on a full-bridge phase-shift PWM DC-DC converter to achieve soft switching (Fig. 1). The main switches are $S1$, $S2$, $S3$ and $S4$. The soft switching technique makes use of the resonance between the intrinsic capacitance of two semiconductor switches and an inductor on the commutation cell. So two ZVS-PWM cells are used; the first cell is composed by the auxiliary switches $Sa1$ and $Sa4$ with the inductor lre , and the second one by $Sa2$ and $Sa3$ with the inductor lrd . Each cell has also one autotransformer (Ae and Ad on Fig. 1), with the same winding ratio Ns/Np and denoted by a . The main switches operate as dual thyristors, achieving zero-voltage switching (ZVS), while the auxiliary switches operate at zero-current switching (ZCS) condition. The processed power is delivered to the load by the power transformer TL and two diodes $Dr1$ and $Dr2$. On Fig. 1 the load is represented by a current source Io . The power processed by the auxiliary circuitry is reduced, because they act only at the switching interval. The power transformer is represented including its leakage inductance Ld .

2. Principle of Operation

In this converter the power is transferred to the load by the displacement between the drives of the diagonalized switches, in this way obtaining an equivalent PWM signal. The two arms of the converter work under

different operating conditions. For the drive sequence shown on Fig. 3, the commutation of the main switches on the left arm always occurs when the converter advance from the power transfer stage to the free-wheeling stage. This commutation process is aided by the load current. The power transfer stage will be called the *active stage*, and the free-wheeling state the *passive stage*. The commutation of the switches on the right arm is achieved when the converter advances from the passive stage to the active stage. During this commutation, the load current flows through the rectifier diodes $Dr1$ and $Dr2$. As a consequence, under such condition the auxiliary circuit should provide the energy required for the commutation process; for that reason, this commutation process will be called a *critical commutation*.

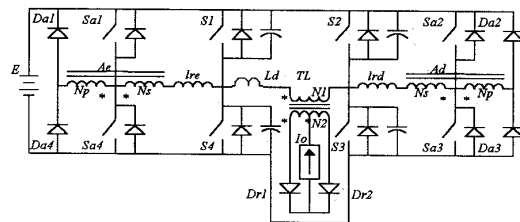


Fig. 1: Proposed circuit

3. Mathematical Analysis

For the analysis of the operation stages of the converter, the following initial considerations will be postulated:

- The switches have bidirectional characteristic on current, with null conduction resistance and null commutation delays.
- The output filter will be represented by a current source reflected to the primary side of the transformer.
- The power transformer has a winding ratio of $N2/N1$ and a leakage inductance denoted by Ld .
- The autotransformers have a null magnetization inductance and act as voltage sources with polarity alternation. Both autotransformers have the same winding ratio of Ns/Np .
- The drive pulses of the auxiliary switches are synchronized with the drive pulses of the main switches.

The analysis will be carried out for a half cycle of the operation proceeding. The commutation cell is considered, for analysis purpose, as an equivalent circuit with an equivalent inductor lr and a capacitor C . The parameters on Eq. (1) and Eq. (2) are associated with such equivalent circuit:

$$Z_0 = \sqrt{\frac{l_r}{2 \cdot C}} \quad (1)$$

$$\omega_0 = \frac{1}{\sqrt{2 \cdot l_r \cdot C}} \quad (2)$$

In this equivalent circuit, the currents and voltages can be normalized with the general expressions of Eq. (3) and Eq. (4):

¹ This work was performed at the Power Electronics Institute of the Federal University of Santa Catarina, while F. C. Castaldo was a student in the M.Sc. Program of Electrical Engineering, with financial support from the Brazilian Council for Research (CNPq).

$$\bar{i} = \frac{i \cdot Z_0}{E} \quad (3)$$

$$\bar{v} = \frac{v}{E} \quad (4)$$

The load current can be referred to the primary circuit with Eq. (5):

$$I_0' = I_0 \frac{N_2}{N_1} \quad (5)$$

t_0 : At the start of the analysis, the converter is supposed to be on the passive stage, where no power is transferred to the load. The switches $S1$ and $S2$ are on.

t_0 to t_1 : The switch $Sa3$ is gated on. The current through the inductor lrd rises linearly from zero to i_b . The diode $Da2$ is on, in view of the induced polarity on the autotransformer Ad . Eq. (6) determines the time interval of this stage:

$$t_1 - t_0 = \frac{i_b \cdot lrd}{E(1-a)} \quad (6)$$

t_1 to t_2 : In t_1 the switch $S2$ is gated off. The charge on the associated capacitance of $S2$ grows up, while the charge on the associated capacitance of $S3$ decreases. At the beginning of this stage, the energy stored on Ld helps the commutation process, until an inversion on the current through Ld occurs. From the circuit for this stage, an equivalent circuit can be generated, where the main equations are Eq. (7) and Eq. (8):

$$v_C = v_{th}(1 - \cos \omega_0' t) + Z_0'(I_0' + i_b) \sin \omega_0' t \quad (7)$$

$$Z_0' [i_{lrd} - i_{Ld}] = Z_0'(I_0' + i_b) \cos \omega_0' t + v_{th} \sin \omega_0' t \quad (8)$$

The following parameters of the equivalent circuit can be defined:

$$v_{th} = \frac{E(1-a)Ld}{lrd + Ld} \quad (9)$$

$$L_{eq} = \frac{lrd \cdot Ld}{lrd + Ld} \quad (10)$$

$$Z_0' = \sqrt{\frac{L_{eq}}{2 \cdot C}} \quad (11)$$

$$\omega_0' = \frac{1}{\sqrt{2 \cdot L_{eq} \cdot C}} \quad (12)$$

$$i_{Leq} = i_{lrd} - i_{Ld} \quad (13)$$

The time interval for this stage can be calculated, thereafter, by Eq. (14):

$$t_2 - t_1 = \frac{\alpha}{\omega_0'} \quad (14)$$

On Eq. (14), α is obtained from Eq. (15):

$$2 \cdot I_0' \cdot \omega_0' \cdot Ld = v_{th}(\alpha - \sin \alpha) + Z_0'(I_0' + i_b)(1 - \cos \alpha) \quad (15)$$

On t_2 , the voltage across the capacitor $C3$ and the current on inductor lrd can be calculated with Eq. (16) and Eq. (17):

$$i_{lrd_0} = I_0' + (I_0' + i_b) \cos \alpha + \frac{v_{th}}{Z_0'} \sin \alpha \quad (16)$$

$$v_{C_0} = v_{th}(1 - \cos \alpha) + Z_0'(I_0' + i_b) \sin \alpha \quad (17)$$

Eq. (16) and Eq. (17) can be normalized, resulting in Eq. (18) and in Eq. (19):

$$\overline{i_{lrd_0}} = \frac{i_{lrd_0} \cdot Z_0}{E} \quad (18)$$

$$\overline{v_{C_0}} = \frac{v_{C_0}}{E} \quad (19)$$

t_2 to t_3 : The current through Ld is clamped at the value of the load current reflected to the primary circuit. As a consequence, at the end of this interval the switch $S3$ shows a zero-voltage commutation. The main equations of this stage are Eq. (20) and Eq. (21):

$$\overline{i_{lrd}} = \overline{I_0'} + (\overline{i_{lrd_0}} - \overline{I_0'}) \cos \omega_0 t + (1 - a - \overline{v_{C_0}}) \sin \omega_0 t \quad (20)$$

$$\overline{v_C} = 1 - a - (1 - a - \overline{v_{C_0}}) \cos \omega_0 t + (\overline{i_{lrd_0}} - \overline{I_0'}) \sin \omega_0 t \quad (21)$$

From Eq. (20) and Eq. (21), the Eq. (22) can be obtained, showing the condition for the zero-voltage commutation for any load current:

$$\overline{i_{lrd_0}} - \overline{I_0'} > \sqrt{|2a - 1 + 2(1-a) \cdot \overline{v_{C_0}} - \overline{v_{C_0}}^2|} \quad (22)$$

t_3 to t_4 : The resonant inductor lrd is demagnetized through the autotransformer, delivering the stored energy back to the primary source E . Once the inductor lrd is completely demagnetized, the switch $Sa3$ can be opened under zero current. The time interval of this stage can be calculated with Eq. (23):

$$\omega_0 \cdot (t_4 - t_3) = \frac{\overline{I_0'} + \sqrt{(\overline{i_{lrd_0}} - \overline{I_0'})^2 + (1 - a - \overline{v_{C_0}})^2 - a^2}}{a} \quad (23)$$

t_4 to t_5 : During this stage the energy is transferred to the load. The switches $S1$ and $S3$ conduct the load current. The duty cycle is given by Eq. (24) and the average load voltage is calculated by Eq. (25):

$$D = \frac{t_5 - t_4}{T_s/2} = 2 \cdot f_s \cdot (t_5 - t_4) \quad (24)$$

$$V_0 = D \cdot E \cdot \frac{N_2}{N_1} \quad (25)$$

t_5 to t_6 : At this stage the converter is advanced from the active state to the passive state. For that, the switch $S1$ is gated off, while $Sa4$ is gated on; the diode $Da1$ goes to conduction mode. As a result, the commutation process is performed under constant load current. At t_6 , the switch $S4$ commutates under zero voltage. An equivalent circuit for this stage leads to the following equations:

$$\overline{i_{lr}} = (1 - a) \sin \omega_0 t - \overline{I_0'}(1 - \cos \omega_0 t) \quad (26)$$

$$\overline{v_C} = (1 - a)(1 - \cos \omega_0 t) + \overline{I_0'} \sin \omega_0 t \quad (27)$$

The circuit analysis shows that the turn's ratio of the autotransformer must be:

$$0,2 < a < 0,5$$

The time interval for this stage is calculated with Eq. (28):

$$\omega_0 \cdot (t_6 - t_5) = \cos^{-1} \frac{\overline{I_0'} \sqrt{1 - 2a + \overline{I_0'}^2 - a(1-a)}}{\overline{I_0'}^2 + (1-a)^2} \quad (28)$$

t_6 to t_7 : At the end of the commutation process, the load begins a free-wheeling state, while the resonant inductor lr is demagnetized through the autotransformer. When the inductor lr is completely demagnetized, the switch $Sa4$ can be gated off under zero-current condition. The time interval for the free-wheeling stage is calculated by Eq. (29):

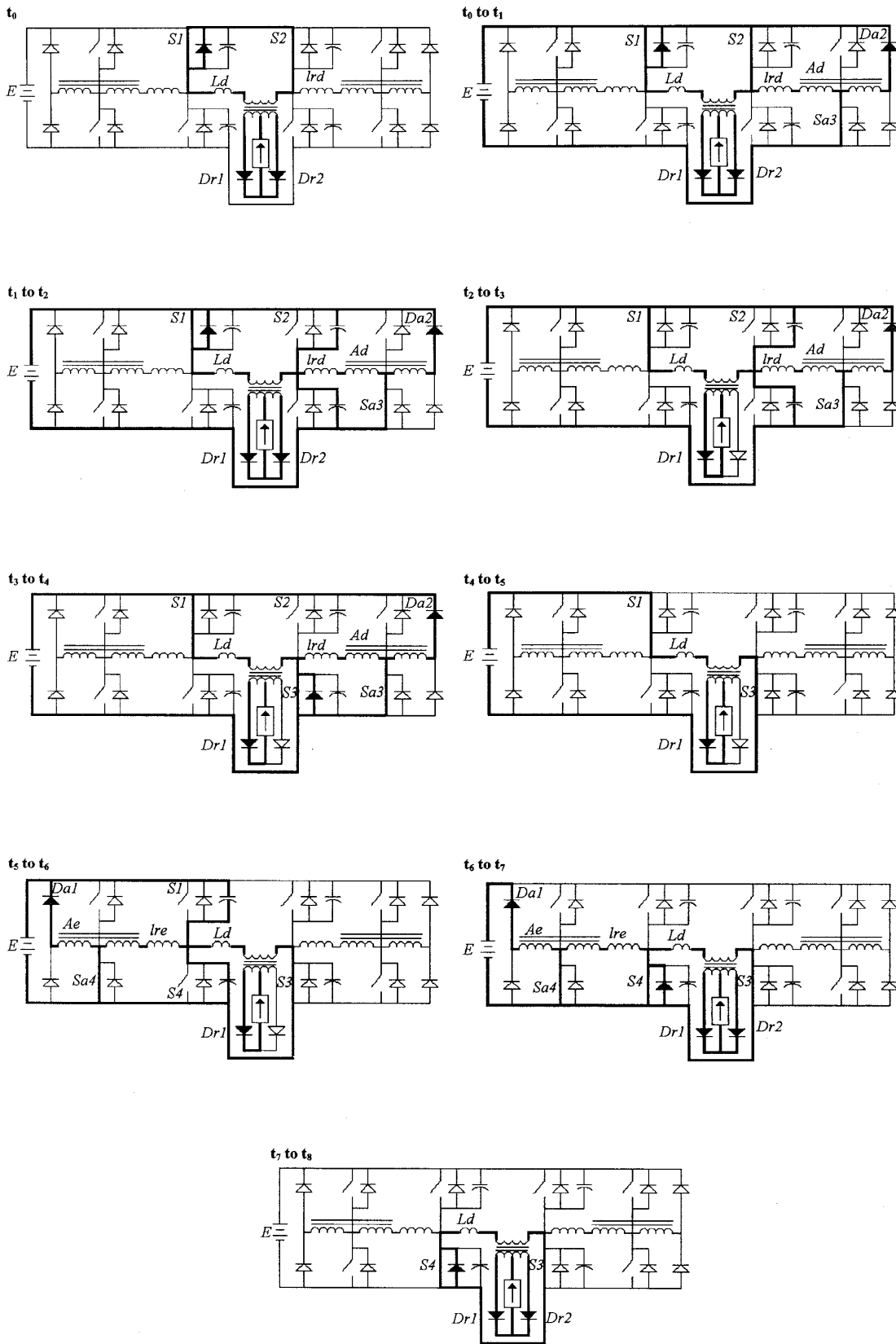


Fig. 2: Operation Stages of the Converter.

$$w_0(t_7 - t_6) = \frac{1-a}{a} \sin^{-1} \cos^{-1} \frac{\overline{I_o'} \sqrt{1-2a + I_o'^2} - a(1-a)}{I_o'^2 + (1-a)^2} + \frac{\overline{I_o'} (1 - \frac{\overline{I_o'} \sqrt{1-2a + I_o'^2} - a(1-a)}{I_o'^2 + (1-a)^2})}{a} \quad (29)$$

t_7 to t_8 : The converter is on the free-wheeling state, the switches $S3$ and $S4$ are on, and no power is transferred to the load. The time interval for that stage is calculated with Eq. (30):

$$t_7 - t_8 = \frac{1-D}{2f_s} \quad (30)$$

As a result of the commutation process, the main switches of the converter are subjected to additional current stresses. Those stresses, on the right arm switches, can be calculated with Eq. (31):

$$i_{add_{rms}} = i_b \cdot \sqrt{\frac{f_s \cdot (t_1 - t_0)}{3}} \quad (31)$$

4. Main Waveforms of the Converter

Fig. 3 shows the main waveforms for a half-cycle operation of the converter.

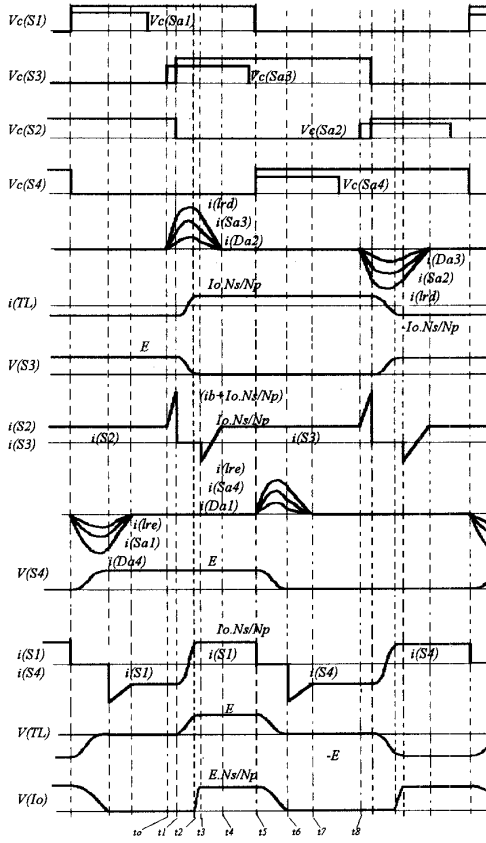


Fig. 3: Main Waveforms of the Converter.

5. Design Procedures

5.1. Design of the Resonant Components

The design of the resonant components begins with the definition of a suitable commutation interval for the main switches, denoted by (t_6-t_7) .

The resonant frequency of the commutation cell is calculated with Eq. (32):

$$f_0 = \frac{\cos^{-1} \left(\frac{-a}{1-a} \right)}{2 \cdot \pi \cdot (t_6 - t_5)} \quad (32)$$

With the value of the resonant frequency obtained from Eq. (32), and an estimate of the intrinsic capacitance of the switches, the inductance of the resonant inductors can be calculated by Eq.(33).

$$L = \frac{1}{8 \cdot \pi^2 \cdot C \cdot f_0^2} \quad (33)$$

5.2. Design Curves

It can be demonstrated that the main stresses on the commutation cells are presented when the converter operates at a no-load condition [8]. From the initial current level i_b , the graphs on Fig. 4, 5, 6 and 7 can be used to obtain the stresses' data on the cell components. Eq. (34) to Eq. (38) should be used for calculation of current levels on the cell components.

$$\overline{i_{Sa_{pk}}} = (1-a) \overline{i_{lr_{pk}}} \quad (34)$$

$$\overline{i_{Da_{pk}}} = a \cdot \overline{i_{lr_{pk}}} \quad (35)$$

$$\overline{i_{Da_{av}}} = \frac{a}{2} \cdot \overline{i_{lr_{av}}} \quad (36)$$

$$\overline{i_{Sa_{rms}}} = \frac{1-a}{\sqrt{2}} \overline{i_{lr_{pk}}} \quad (37)$$

$$\overline{i_{Sa_{pk}}} = (1-a) \overline{i_{lr_{pk}}} \quad (38)$$

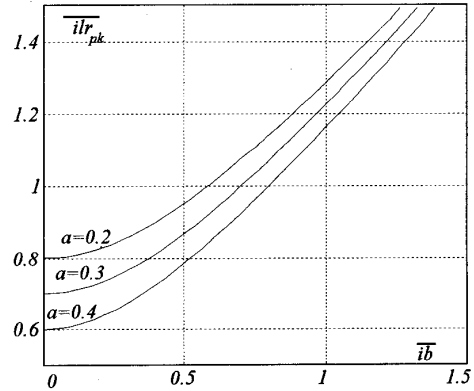


Fig. 4: Peak value of the current through the resonant inductors.

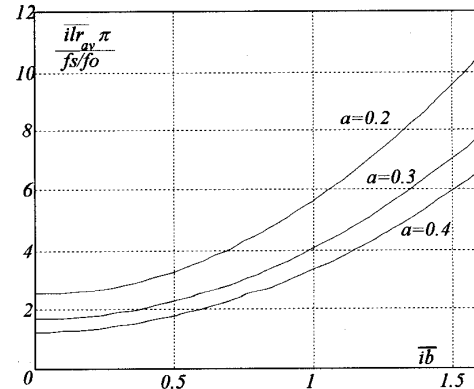


Fig. 5: Average value of the current through the resonant inductors.

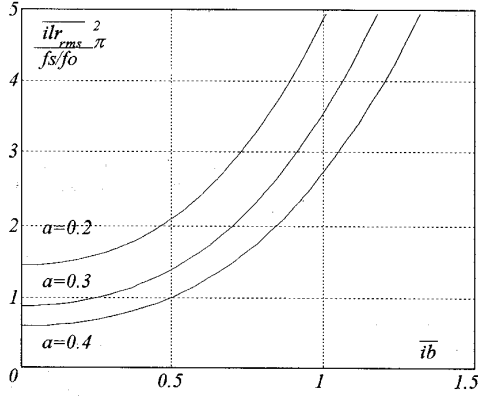


Fig. 6: RMS values of the current through the resonant inductors.

The conduction interval of the commutation cell is obtained from Fig. 7, where Δt_{total} is $(t_4 - t_0)$ for the right arm cell and $(t_7 - t_5)$ to the left arm cell.

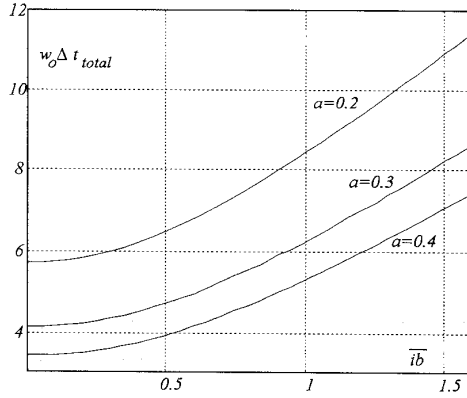


Fig. 7: Conduction interval for the commutation cells.

5.3. Design Example

A prototype rated 1500 W was built to evaluate the proposed circuit. MOSFETs were used for the main and auxiliary switches. Other characteristics of the prototype were:

- DC input voltage: 300 V
- DC output voltage: 60 V
- DC output current at full load: 25 A
- Switching frequency: 75 kHz
- Autotransformer voltage ratio: 3:1
- Efficiency: about 0.9
- Power Transformer voltage ratio $N1/N2$: 16/4
- Transformer Leakage Inductance: 2.3 μH
- Capacitance of the Switches: 3.5 nF

The autotransformers turns ratio (a) was chosen as 0.3 as used in [3] and [4]. The resonant frequency is calculated with Eq. (32), using $(t_6 - t_5) = 500$ ns and resulting in $f_o = 640$ kHz. With this value and the switches' capacitance, the inductance of the resonant inductors can be obtained by Eq. (33), resulting in $l_r = 10 \mu H$.

The Z_o parameter is calculated thereafter with Eq. (1), resulting in $Z_o = 37.8 \Omega$.

With the resonant components of the commutation cell, the current i_b is calculated, using the following parameters:

$$\begin{aligned} E &= 300V \\ l_r &= 10 \mu H \\ C &= 3.5 nF \\ L_a &= 2.3 \mu H \\ I_o'_{Nom} &= 6.25 A \end{aligned}$$

Using Eq. (9) to Eq. (12), it is obtained:

$$\begin{aligned} v_{th} &= 39.26 V \\ L_{eq} &= 1.87 \mu H \\ Z_o' &= 16.3 \Omega \\ \omega_o' &= 8.74 \times 10^6 \text{ rd/s} \end{aligned}$$

The commutation process should be verified for a range of the output current, from the no-load condition to full-load. Using Eq. (15) to Eq. (19) and Eq. (22), in an iterative process, it is obtained $\overline{ib} = 9$ A.

The current i_b can be normalized with Eq. (3), resulting: $\overline{i_b} = 1.15$ A.

From the design graphs on Fig. 4, 5 and 6, the r.m.s., average and peak values of the current through the resonant inductor are:

$$\overline{ilr_{rms}} = 0.48 pu \therefore ilr_{rms} = 3.8 A$$

$$\overline{ilr_{avg}} = 0.24 pu \therefore ilr_{avg} = 1.9 A$$

$$\overline{ilr_{pk}} = 1.34 pu \therefore ilr_{pk} = 10.5 A$$

The r.m.s. and peak values of the current through the auxiliary switches are calculated with Eq. (34) to Eq. (38):

$$\overline{isa_{rms}} = \frac{1-a}{\sqrt{2}} \overline{ilr_{rms}} = 0.23 pu \therefore isa_{rms} = 1.8 A$$

$$\overline{isa_{pk}} = (1-a) \overline{ilr_{pk}} = 0.94 pu \therefore isa_{pk} = 7.4 A$$

On the same way, the average and peak values of the current through the auxiliary diodes are:

$$\overline{ida_{avg}} = \frac{a}{2} \overline{ilr_{avg}} = 0.04 pu \therefore ida_{avg} = 0.3 A$$

$$\overline{ida_{pk}} = a \overline{ilr_{pk}} = 0.4 pu \therefore ida_{pk} = 3.2 A$$

The conduction interval of the commutation cell is used to design the autotransformers and the resonant inductors. The graph on Fig. 6 is used to find:

$$\Delta t_{total} = (t_4 - t_0) = 2 \mu s$$

The same process is used for the design of the left arm elements. It should be notice, however, that $\overline{ib} = 0$ for the left arm commutation cell. The following results were obtained:

$$\overline{ilr_{rms}} = 0.21 pu \therefore ilr_{rms} = 1.65 A$$

$$\overline{ilr_{avg}} = 0.08 pu \therefore ilr_{avg} = 0.6 A$$

$$\overline{ilr_{pk}} = 0.7 pu \therefore ilr_{pk} = 5.5 A$$

$$\overline{isa_{rms}} = \frac{1-a}{\sqrt{2}} \overline{ilr_{rms}} = 0.10 pu \therefore isa_{rms} = 0.8 A$$

$$\overline{isa_{pk}} = (1-a) \overline{ilr_{pk}} = 0.49 pu \therefore isa_{pk} = 3.9 A$$

$$\overline{ida_{avg}} = \frac{a}{2} \overline{ilr_{avg}} = 0.01 pu \therefore ida_{avg} = 0.1 A$$

$$\overline{ida_{pk}} = a \overline{ilr_{pk}} = 0.21 pu \therefore ida_{pk} = 1.6 A$$

$$\Delta t_{total} = (t_7 - t_5) = 1 \mu s$$

In practice, the same elements calculated for the right arm can be used on the left arm of the converter.

Using Eq. (31) the additional current stresses on the switches can be calculated, resulting:

$$i_{add_rms} = 1A$$

As a consequence, the switches on the left arm of the converter should be selected using the following values:

$$i_{S1_rms} = i_{S4_rms} = \frac{I_o'}{\sqrt{2}} = 4,41A$$

For the right arm switches, the current values are:

$$i_{S2_rms} = i_{S3_rms} = \sqrt{4,4^2 + 1^2} = 4,5A$$

It should be notice that the peak current on the right arm switches is calculated by:

$$i_{S2_pk} = i_{S3_pk} = i_b + I_o' = 15,25A$$

6. Experimental Results

Bench tests with the prototype demonstrate that the switches can operate at high frequency with soft commutation over an extended load range, from no-load to full load condition.

The current and voltage on the main switches of the right arm are shown on Fig. 8. On the current signal it is noticed the additional current due to the commutation cell. On Fig. 9 it is shown a detailed view of the same signals, showing the zero voltage switching.

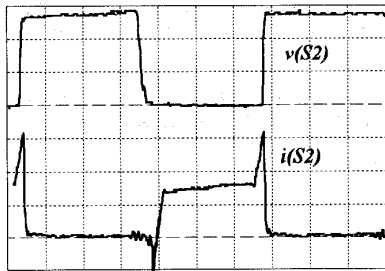


Fig. 8: Zero-voltage switching on S2.
Scales: Voltage = 100 V/div; Current = 5 A/div;
Time = 2 μs/div

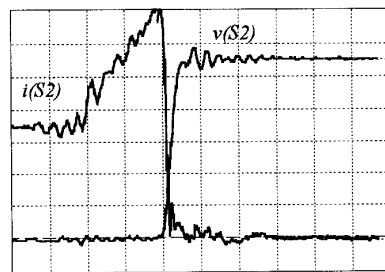


Fig. 9: Detail of the Zero-voltage switching on S2.
Scales: Voltage = 50 V/div; Current = 2 A/div;
Time = 2 μs/div

On Fig. 10, it is shown the voltage and current on the switches of the left arm. The switches commutates under zero-voltage and without additional current stresses.

Fig. 11 shows the commutation under zero-current on the auxiliary switches of the right arm.

The waveforms of voltage and current on the primary windings of the power transformer is shown on Fig. 12.

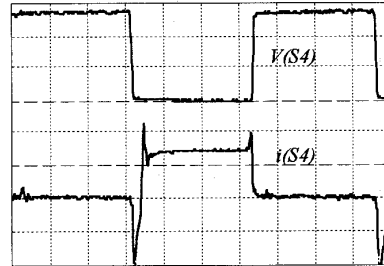


Fig. 10: Zero-voltage switching on S4.
Scales: Voltage = 100 V/div; Current = 5 A/div;
Time = 2 μs/div

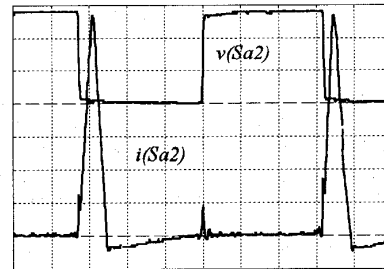


Fig. 11: Zero-current switching on Sa2.
Scales: Voltage = 100 V/div; Current = 1 A/div;
Time = 2 μs/div

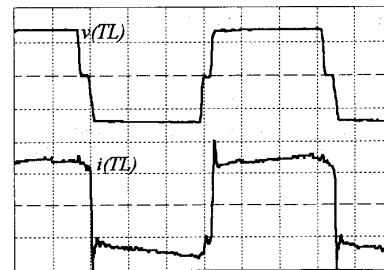


Fig. 12: Voltage and current on the transformer TL.
Scales: Voltage = 200 V/div; Current = 5 A/div;
Time = 2 μs/div

Fig. 13 shows the output voltage of the prototype as a function of the output current, for several values of duty cycle of the switches. It is noticed that the converter behaves as a constant voltage source for an extended power range.

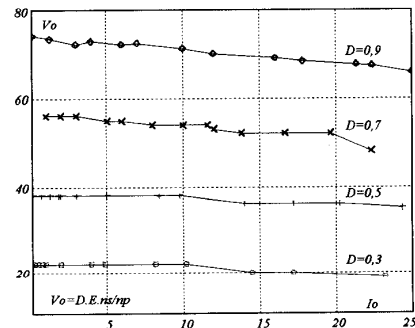


Fig. 13: Output characteristic of the prototype.

The prototype efficiency is shown in Fig. 14. The maximum measured efficiency was 93 %, at the full load condition.

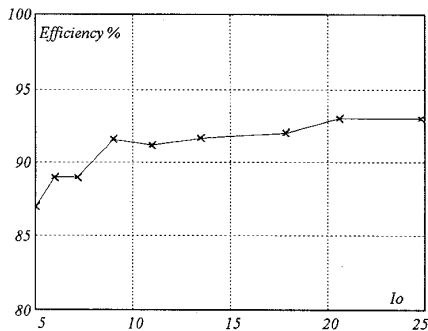


Fig. 21: Prototype efficiency.

7. Conclusions

The ZVS-PWM commutation cell was applied to a Full-Bridge PWM DC-DC Converter. Evaluation of a prototype based on the new circuit showed that the proposed circuit has some distinguished characteristics:

- The commutation losses are minimum, because the main switches operate under zero-voltage condition, and the auxiliary switches at zero-current condition.
- The current through the auxiliary switches is present only for a short interval during the commutation cycle; as a result, the conduction losses on those switches and on the associated devices are kept on a small value.
- The proposed circuit behaves as a constant voltage source for an extended range of output current. That characteristic can be a requisite in many industrial applications.
- The ZVS and ZCS characteristics of the switches are present on all load condition of the converter.
- No voltage stresses were detected across the switches.
- The efficiency of the converter was very high.
- The commutation process can be employed with any of the known power switches' technologies, such as IGBTs, GTOs and BJTs.

As a result of such characteristics, it can be concluded that the proposed converter is specially suitable for high power applications.

References

- [1] H. Foch, Y. Cheron, M. Metz and T. Meynard. **Commutation mechanisms and soft commutation in static converters**, *2nd Brazilian Power Electronics Conference*, December 1991, pp. 338-346.
- [2] I. Barbi and D. C. Martins. **A true PWM zero-voltage switching pole with very low additional RMS current stress**, *Proceeding of the PESC '91*, pp. 261-267.
- [3] D. C. Martins, J. A. Brilhante and F. M. Seixas. **Buck PWM Converter using a new ZVS commutation cell**, *2nd Brazilian Power Electronics Conference*, November-December 1993, pp. 93-98.
- [4] D. C. Martins, F. M. Seixas, J. A. Brilhante and I. Barbi **A family of DC-DC PWM converters using a new ZVS commutation cell**, *Proceeding of the PESC '93*.
- [5] J. G. Cho, J. L. Sabaté and F. C. Lee **A novel full-bridge zero voltage transition PWM DC-DC converter for high power applications**, *Proceeding of the APEC '94*, pp. 143-149.
- [6] G. Hua, C. S. Leu and F. C. Lee. **Novel zero-voltage transition PWM converters**, *Proceeding of the PESC '92*, pp. 55-61.
- [7] F. M. Seixas. **Analysis of the ZVS-PWM-GEPAE commutation cell and its application on DC-DC and DC-AC converters**, *Master's Thesis - Federal University of Santa Catarina*. 1993. (in Portuguese).
- [8] F. C. Castaldo. **Study of the DC-DC Full-Bridge converter with the ZVS-PWM-GEPAE auxiliary commutation cell**, *Master's Thesis - Federal University of Santa Catarina*. 1994. (in Portuguese).